Dynamics and reversibility of oxygen doping and de-doping for conjugated polymer

Hua-Hsien Liao, Chia-Ming Yang, Chien-Cheng Liu, Sheng-Fu Horng, Hsin-Fei Meng, and Jow-Tsong Shy

Citation: Journal of Applied Physics **103**, 104506 (2008); doi: 10.1063/1.2917419
View online: http://dx.doi.org/10.1063/1.2917419
View Table of Contents: http://scitation.aip.org/content/aip/journal/jap/103/10?ver=pdfcov
Published by the AIP Publishing

Dynamics and reversibility of oxygen doping and de-doping for conjugated polymer

Hua-Hsien Liao,[1] Chia-Ming Yang,[1] Chien-Cheng Liu,[1] Sheng-Fu Horng,[1] Hsin-Fei Meng,[2,a)] and Jow-Tsong Shy[3]
[1]*Department of Electric Engineering, National Tsing Hua University, Hsinchu 300, Taiwan, Republic of China*
[2]*Institute of Physics, National Chiao Tung University, Hsinchu 300, Taiwan, Republic of China*
[3]*Department of Physics, National Tsing Hua University, Hsinchu 300, Taiwan, Republic of China*

(Received 12 December 2007; accepted 3 March 2008; published online 23 May 2008)

We perform comprehensive long-time monitoring of the *p*-doping and de-doping of poly(3-hexyl thiophene) under changing external conditions of oxygen, light, and temperature. They are shown to be controlled by the complex adsorption and desorption process with time scales ranging from seconds to weeks. The oxygen doping at atmospheric pressure takes several hours in the dark. The doping is dramatically accelerated to be within seconds with light of wavelength of 500–700 nm. Even at low oxygen pressure of 10^{-4} torr doping occurs within minutes with light. The de-doping by oxygen desorption takes as long as weeks at room temperature and vacuum of 10^{-4} torr, but when the temperature is raised to near the polymer glass temperature of 370 K, the de-doping is accelerated to minutes as the enhanced chain motion releases the trapped oxygen. Even though visible and near infrared light causes very efficient doping within seconds or minutes depending on vacuum level, such light-induced doping is not a chemical reaction and is fully reversible by thermal annealing at the end without sacrificing the mobility. For the polymer field-effect transistors, only the carrier density is changed while the mobility remains roughly a constant for all the conditions.
 [DOI: 10.1063/1.2917419]

I. INTRODUCTION

Flexible electronics is the next generation technology which has received considerable attention recently. Conjugated polymers have been viewed as the most promising material due to their easy fabrications and remarkable optoelectronic properties. Polythiophenes are one class of conjugated polymers intensively studied due to their excellent performance in field-effect transistors (FETs)[1] and solar cells,[2,3] especially for poly(3-hexylthiophene) (P3HT). However, the high off-current, defined as the source-drain current at zero gate bias for a FET, delays their progress towards commercialization. A FET with high off-current has a low on/off-current ratio.[4] Such off-current also contributes an ohmic component to the solar cell and reduces the open-circuit voltage.[5,6] Therefore, reducing the off-current of P3HT is a key issue for FETs and solar cells. It was known that oxygen is responsible for the *p*-doping,[7–10] which causes the off-current. The oxygen doping and de-doping processes depend on a variety of physical factors such as temperature, light, and vacuum.[4,11–17] Abdou *et al.* reported O_2 causes P3HT *p*-doping through charge transfer complex states and the doping is reversible by using vacuum.[7] Thermal treatment is also shown to de-dope P3HT FET.[4] O_2 doping effect is found to be enhanced by light and it appears that this photo-induced doping effect is persistent and can be used as a new doping method.[12] So far the dynamics of the doping process is not given and how the steady state is reached after the physical factor changes remains unclear. In addition to the dynamics of the oxygen doping process, the reversibility of the doping is a key question both from the fundamental and practical points of view. Only recently has it been understood that the P3HT dark oxygen doping process is a physical adsorption for oxygen on P3HT (Ref. 18) rather than a chemical reaction. One would therefore expect a full reversibility of oxygen doping after de-doping in vacuum. On the other hand, ambient light is known to significantly enhance the oxygen doping, which may result from some irreversible photo-chemical reactions common for organic semiconductors. On the practical side, the fabrication for polymer electronics also greatly depends on whether the doping is reversible or not as some levels of oxygen and light are inevitable in the fabrication. If reversible, the fabrication process does not need to be very strict on the environment control since the unwanted doping can be removed at the end by a de-doping step. On the other hand, if the doping is irreversible, every step of the process must be under strict control and the fabrication cost will be much higher. Despite a considerable number of reports on the sensitivity of P3HT and other conjugated polymers on oxygen at various temperature and illumination conditions, so far the full dynamics of the oxygen doping and de-doping process under changing physical environment is not mapped out and the reversibility remains unknown.

In this work using two-terminal conductivity and three-terminal field-effect transistor measurements we perform a long-time monitoring of the doping level of P3HT under a series of physical environments with different temperatures, oxygen pressures, vacuum levels, as well as light intensities

a)Author to whom correspondence should be addressed. Electronic mail: meng@mail.nctu.edu.tw.

and wavelengths. How the system approaches the steady state at each stage is recorded and the entire history of all the behaviors during several days is mapped out. It turns out the different processes are controlled by different time scales ranging from minutes to as long as days. In particular, no matter how heavily P3HT is doped, it is always reversible under heat treatment in vacuum if one waits long enough, with the only exception of illumination under an ultraviolet laser in the presence of oxygen. The process can be repeated in infinite cycles. A full picture is therefore established for the complex yet reversible physical interaction between molecular oxygen and P3HT films, which involves processes such as the diffusion through the polymer matrix, adsorption in the dark or facilitated by light, desorption at room temperature, and desorption above glass temperature.

II. EXPERIMENTAL PROCEDURE

In a two-terminal source-drain device (SD) Au electrodes are defined by a shadow mask with 50 μm channel length and 2 mm width on a glass substrate. The P3HT is purchased from Aldrich and dissolved in chloroform with 1 wt % for spin-coating on the previously patterned glass substrate in air to form a 1000 Å P3HT film. Each glass substrate has eight SD devices to check the experiment consistence. The three-terminal source-drain-gate transistor device is fabricated as in a previous report.[1] The P3HT film is spin-coated like the SD device without a self-assemble monolayer. The sample is placed in a JANIS CCS-150 closed cycle system with a temperature controlled system. The closed cycle system is pumped by a Leybold turbo pumping station. Different pressure gauges are used to monitor the pressure in different ranges, including the Leibold TTR 91 vacuum gauge and MKS Baratron® 722 absolute vacuum gauge. *I-V* curves are measured by two Keithley 2400 controlled by Labview programs. I_{sd} is measured once every 5 s, and the voltage is only applied on the sample during the I_{sd} measurement. All of our I_{sd} time-evolution data are measured by this intermittent method to avoid the effect of mobile ionic impurities from the glass substrate.[19]

Light from a 250 W quartz-tungsten-halogen lamp passing through a monochromator is focused into the chamber on the sample. The monochromated light intensity is measured by a calibrated Si detector to calculate the relative photon flux n_p. I_{sd} increment, ΔI_{sd}, was measured under a monochromated light illumination with a constant illumination time Δt. The photo-induced oxygen doping rate is proportional to $\Delta I_d/\Delta t n_p$.

III. RESULTS AND DISCUSSIONS

A. Oxygen effect of two-terminal devices

A two-terminal source-drain (SD) device with 50 μm channel length is used. The off-current I_{sd} between the drain and source electrodes is measured for V_{SD} voltage from −200 to +200 V. The current-voltage curve is symmetric and linear, indicating that the current is determined by the bulk conductivity rather than the interface effect.[20,21] Intermittent current measurement is used during the long monitoring period to avoid the mobile ionic effect from the glass substrate.[19] For fixed carrier mobility, I_{sd} is proportional to the carrier density due to doping. Figure 1 shows the I_{sd} dynamics of a two-terminal P3HT SD device at 200 V under different conditions, and Table I summarizes the results. Initially, I_{sd} is 506 nA after a short exposure to air following the P3HT film deposition by spin-coating. When the sample is placed in dark vacuum (10^{-4} torr) at 300 K for 23 h (Procedure 1–1), I_{sd} is gradually reduced from 506 to 115 nA, consistent with the previous report that long time in vacuum causes O_2 de-doping.[7] Decrease of I_{sd} is very slow and nonexponential, so it is difficult to reduce the off-current substantially by vacuum alone. Therefore the device is heated at 370 K for 5.7 h in the dark vacuum (Procedure 1–2). After a sudden rise due to an increase of mobility, I_{sd} starts to decrease at 370 K. After cooling back to 300 K, I_{sd} goes further down to 9 nA. Such low current level might be achieved by vacuum at 300 K as well, but it must take several days, even weeks.

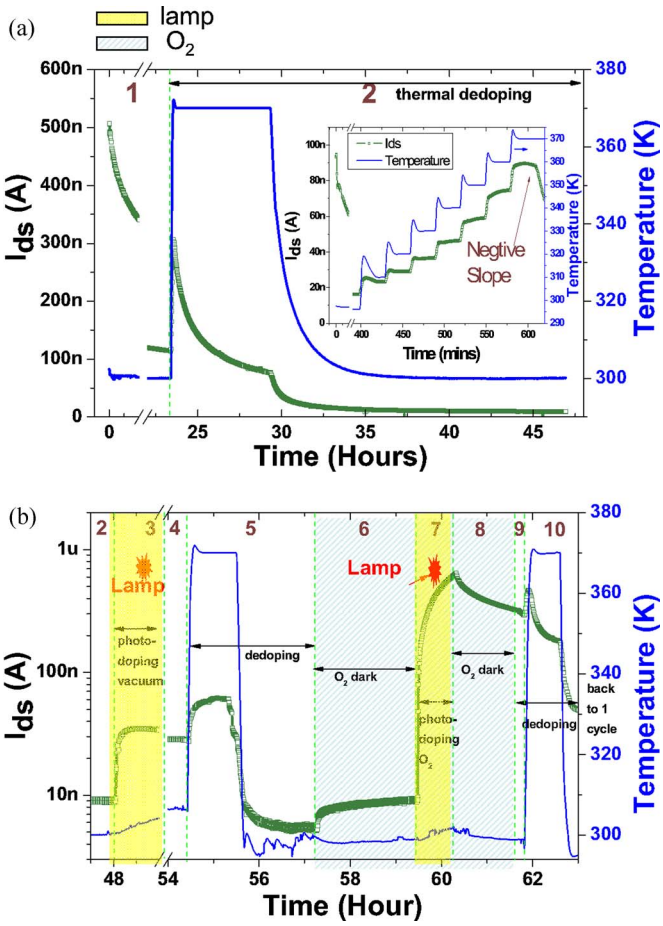

FIG. 1. (Color online) The time evolution of the dark current I_{ds} of a two-terminal DS device. (a) is from 0 to 47 h and (b) is from 47 to 63 h. The inset of (a) is the dark current at I_{ds} with different annealing temperatures for two DS devices at V_{DS}=200 V. Table I summarized I_{ds} at different procedures on the figures. The yellow regions are under lamp illumination and green shaded regions are under high O_2 pressure.

After the thermal annealing, we study the light effect on I_{sd} under vacuum. The light of a fluorescent lamp is introduced into the vacuum chamber without focusing through the optical window of the closed-cycle cryogenic system (Procedure 1–3). The illumination lasts for 6.4 h. I_{sd} initially

TABLE I. Time-correlated current of source-drain devices at different experimental conditions.

Procedure	Time interval (h)	Light	Temperature (K)	O_2	Initial current (nA)	Final current (nA)
1	0–23	Dark	300	Vacuum	506	115
2	23–48	Dark	370 for 5.7 h	Vacuum	115	9
3	48–48.3	Light for 0.3 h	300	Vacuum	9	35
4	48.3–54.4	Dark	300	Vacuum	35	28
5	54.4–57	Dark	370 for 1 h	Vacuum	28	5.2
6	57–59.4	Dark	300	650 torr for 2 h	5.2	8.7
7	59.4–60.3	Light for 0.83 h	300	125 torr	8.7	628
8	60.3–61.5	Dark	300	125 torr for 1.2 h	628	328
9	61.5–61.7	Dark	300	Vacuum	328	290
10	61.7–63	Dark	370 for 1 h	Vacuum	290	11

increases from 9 to 35 nA within 20 min, then saturates for the next 6 h. The increased current is not a band-gap transition photocurrent because when the light is removed I_{sd} does not return to the original level rapidly. Even in the vacuum below 10^{-4} torr I_{sd} is still increased four times by the light within a short time interval, contrary to the previous assumptions.[12,13] After a 370 K annealing for 1 h (Procedure 1–5), I_{sd} is reduced to 5 nA, which is slightly lower than the current before Procedure 1–2, demonstrating that the photo-induced oxygen doping is reversible. In the subsequent procedures we clarify the correlation of O_2 and light: 650 torr of O_2, about four times the O_2 composition in air, is introduced to the dark chamber at 300 K. After 2 h I_{sd} only increased slightly from 5 to 9 nA with a constant rate of 0.62 nA/h (Procedure 1–6). In other words, oxygen doping in the dark is a very slow process even for high O_2 pressure. O_2 pressure is then lowered from 650 to 125 torr, which is approximately the O_2 composition in air, and the light from the same lamp is introduced into the chamber without focusing (Procedure 1–7). I_{ds} now rapidly increases to 628 nA within 50 min with 743 nA/h increasing rate, which is higher than the initial current value 506 nA. If there were no light to assist, it would take over 42 days to achieve 628 nA with a doping rate 0.62 nA/h by 650 torr of O_2 in the dark. It illustrates that reduced I_{sd} can be rapidly recovered by a photo-induced O_2 doping process. The rise of I_{sd} is faster than in Procedure 1–3 where light is applied under vacuum. From Procedure 1–1 to 1–7, it is obvious that the oxygen-induced *p*-doping is a reversible process.

Note the photo-induced doping in Procedure 1–3 is in a relatively high vacuum of 10^{-4} torr. Contrarily, the photo-induced doping Procedure 1–7 is under an atmospheric O_2 pressure of 125 torr. Because of the potential of photochemical reaction in the presence of both light and oxygen, one might expect that, unlike the reversibility of doping in Procedure 1–3, the doping in Procedure 1–7 becomes irreversible. The reversibility is checked by the subsequent procedures. After Procedure 1–7, light is removed (Procedure 1–8) and, as in Procedure 1–4, I_{sd} does not disappear immediately but gradually decreases in the dark with 125 torr O_2 atmosphere at 300 K, showing the substantially increased I_{sd} up to nearly 1 μA does not come from the band-gap transition photocurrent but from O_2 doping. Procedures 1–9 and 1–10 in Fig. 1(a) are vacuum and annealing processes, respectively, and they reduce I_{sd} just like Procedures 1–2 and 1–5. It is not shown here but was verified several times that I_{sd} can return to a very low level of a few nA as in Procedure 1–2, if the vacuum annealing time is tens of hours as the case of Procedure 1–2. The results demonstrate that even in the coexistence of high oxygen pressure and light, there is no chemical reaction and the photo-induced doping remains physical in nature and reversible under subsequent vacuum annealing. From Procedures 1–2 and 1–10, it is clear that de-doping is much more efficient at 370 K than at 300 K. The temperature dependency of the de-doping is studied by varying the temperature step by step. I_{sd} at different annealing temperatures are shown in the inset of Fig. 1(a). The sample starts with a reduced doping level after staying in dark vacuum over 6 h at 300 K. As the temperature rises I_{sd} increases due to the higher mobility. However, as the temperature is raised to 370 K, I_{sd} develops a negative slope with time indicated by the arrowhead in the inset of Fig. 1(a). Note 370 K is near the glass temperature of P3HT.[22] As we repeat the Procedure 1–1 with the long-time vacuum process for a heavily doped sample at elevated temperature, even at 310 K I_{sd} starts to be reduced more efficiently than at 300 K. This implies that most of O_2 adsorbed on or near the surface of the heavily doped P3HT sample can be easily desorbed by vacuum, and small thermal energy can speed up this desorption process. After these shallowly adsorbed O_2 molecules are removed, the deeply trapped O_2 molecules can only be removed by a high temperature annealing process near the glass temperature of the polymer film. This temperature must be high enough to make P3HT chains mobile and release the O_2 molecules to the surface. The time scales for the doping and de-doping procedures are summarized in Table II. From the table it is seen that interestingly for the oxygen doping

TABLE II. The oxygen doping and de-doping rate at different experimental environments.

Doping condition	Rate
Light+Vacuum	Moderate (~min)
O_2, dark	Slow (~h)
O_2, Light	Fast (~s)
De-doping condition	**Rate**
300 K+Vacuum+Dark	Very slow (~days to weeks)
370 K+Vacuum+Dark	Moderate (~min)

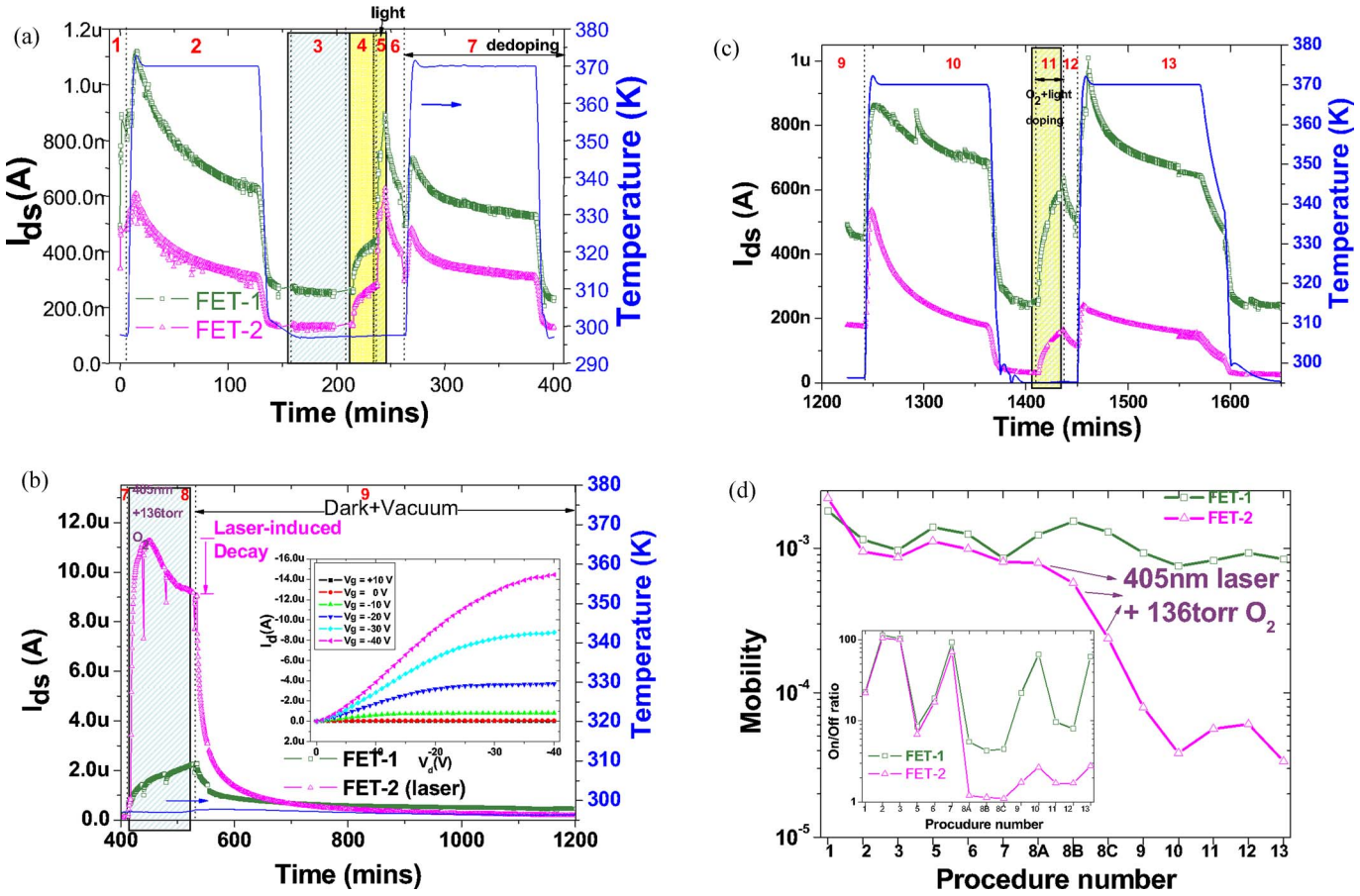

FIG. 2. (Color online) The dark current I_{ds} time evolutions of two FET devices with V_{DS}=−40 V and V_{GS}=0 V. (a) is from 0 to 400 min, (b) is 400 to 1200 min, (c) is 1200 to 1650 min, and (d) is the mobility of two FETs at different procedures. The inset in (d) is the on/off-current ratio at different procedures. The on-current is measured at V_{DS}=−40 V and V_{GS}=−40 V. The off-current is measured at V_{DS}=−40 V and V_{GS}=0 V. These results after different procedures are summarized in Table II. The typical transistor characteristics are shown in the inset of (b).

process the presence of light is more important a factor than the oxygen pressure itself. This suggests that ambient light must be under strict control if a low level of doping is to be maintained throughout that sample fabrication and operation. As for the de-doping, even though the doping can always be undone in vacuum, it will take an extremely long time, up to weeks at room temperature. Raising the temperature to 370 K, close to the glass transition temperature, can accelerate the process significantly to minutes.

B. Oxygen effect of field-effect transistors

So far we measured the current I_{sd}, which is proportional to the product of hole carrier density p and mobility μ, with the assumption that mobility is basically independent of O_2 adsorption so all the changes in current are due to carrier density. Below transistor measurement is carried out to verify this assumption. Two FET devices, FET-1 and FET-2, on the same substrate are monitored in procedures similar to the previous two-terminal device. Besides the off-current I_{sd}, the mobilities and on/off-current ratios of two FETs are also recorded at the same time. The FET off-current I_{sd} is measured at drain-source voltage V_{SD}=−40 V and gate-source voltage V_{GS}=0 V in the dark except for cases to be specified. The off-current I_{sd} is compared to the FET source-drain on-current at V_{SD}=−40 V and V_{GS}=−40 V to get the on/off ratio. The off-currents I_{sd} are shown in Figs. 2(a)–2(c). The mobility of the device is fitted from the source-drain current at V_{SD}=−40 V as a function of V_{GS} using the saturated region formula. The mobility and on/off-current ratio are plotted via procedures in Fig. 2(d). The typical FET characteristics are shown in the inset of Fig. 2(b).

After introducing the sample into the chamber, it is annealed at 370 K in vacuum for 2 h immediately to reduce the oxygen doping (Procedure 2–2). When the temperature is cooled down to 300 K, I_{sd} is decreased to 275 and 175 nA for FET-1 and FET-2, respectively, and the on/off-current ratios for FET-1 and FET-2 are increased five times. At the same time, the field effect mobilities for both transistors decrease only slightly. This demonstrates that the significant decrease of I_{sd} is mainly due to the carrier density p instead of the mobility μ as expected. It also shows that the annealing process at this temperature only enhances the O_2 de-doping to reduce the carrier density but does not degrade the carrier mobility.[4] Next, 650 torr of O_2 is introduced into the dark chamber (Procedure 2–3). The off-current I_{sd}, on/off-current ratios, and carrier mobilities are measured after 50 min. The off-current I_{sd} for FET-1 and FET-2 increases by 1–2 nA. Both on/off-current ratios and carrier mobilities remain about the same. It illustrates that in the dark environment O_2 doping rate remains low even as the O_2 pressure is increased for

several orders of magnitude, consistent with previous results of two-terminal devices shown in Fig. 1. Then the O_2 pressure is reduced to vacuum for 30 min and then raised to 125 torr; the light is also introduced in both O_2 pressures (Procedures 2–4 and 2–5). Within 20 min the I_{sd} of the two devices increases substantially, and the on/off-current ratio decreases over ten times. The carrier mobilities slightly increase. Once again, it shows that the I_{sd} changes were caused by the carrier density variations, not the carrier mobility. I_{sd} increases faster when the light intensity increases. When the light and O_2 are removed, the chamber becomes dark vacuum again and I_{sd} does not disappear immediately but decreases gradually with time (Procedure 2–6). The on/off-current ratios are increased by two times, but the carrier mobilities are only decreased slightly. After a 2 h annealing process at 370 K (Procedure 2–7), I_{sd} and on/off-current ratio are back to the levels before photo-induced O_2 doping in Procedure 2–2. The simultaneous monitoring of both I_{sd} and μ through Procedures 2–1 to 2–7 establishes that all the variations are dominated by the carrier density caused by O_2 doping while the mobility changes little, therefore the procedures are basically reversible. If the annealing time is longer, the off-current I_{sd} will be even lower and the on/off ratio even higher.

Using transistors we show that P3HT O_2 doping and de-doping processes are almost reversible, except for the slightly decreased mobility. We suspect the slightly decreased mobility is caused by the irreversible photo-oxidation due to short-wavelength photon. To check this 136 torr of O_2 is introduced into the chamber, and a 405 nm laser beam is focused on FET-2. FET-1 inevitably receives some scattered laser light. Within 30 min, the off-current I_{sd} of FET-2 is increased by almost 2 orders of magnitude. On the other hand, the dark current of FET-1 is only increased by 1 order of magnitude by the scattered 405 nm light (Procedure 2–8). The on/off ratios are reduced by 17 and 60 times for FET-1 and FET-2, respectively. The mobility of FET-2 starts to decrease upon 405 nm illumination, but the mobility for FET-1 remains the same. The off-current I_{sd} rises sharply for FET-2, indicating strong photo-induced O_2 doping by the 405 nm laser. After 40 min of laser illumination I_{sd} of FET-2 starts to decrease, but I_{sd} of FET-1 remains increasing. From Fig. 2(d) the decrease of I_{sd} of FET-2 is mainly due to its mobility decay. The transistor characteristics are measured three times during Procedure 2–8, indicated by 8A, 8B, and 8C in Fig. 2(d). After 2 h laser illuminations, the chamber is switched to the dark vacuum, and I_{sd} of FET-1 and FET-2 both gradually decrease (Procedure 2–9). FET-2 mobility further decreases as shown in Fig. 2(d). In dark vacuum for a night, I_{sd} of FET-1 and FET-2 decreases, but only the on/off ratio of FET-1 increases slightly. The severe degradation of the mobility of FET-2 compared with FET-1 suggests that the 405 nm laser illumination in the presence of oxygen causes irreversible chemical reactions, which cannot be undone by subsequent physical process. We verify this by the following de-doping procedure: the de-doping by thermal annealing at 370 K for 2 h (Procedure 2–10). While the I_{sd} is reduced the on/off ratio cannot return to the previous level. The mobility of FET-2 remains low after the laser is turned off for a long time (Procedure 2–9) in Fig. 2(d), demonstrating that the laser does cause irreversible damage in Procedure 2–8. The coexistence of O_2 and focused 405 nm laser is therefore identified as the only procedure to break the reversibility of the P3HT system. It is interesting to check whether the laser-damaged P3HT films still have reversible O_2 doping property. A photo-induced O_2 doping and high temperature annealing processes are applied to FET-1 and FET-2 again (Procedures 2–11, 2–12, and 2–13). The 130 torr O_2 and white light from the lamp are introduced into the chamber at the same time, similar to Procedure 2–5. Within 10 min large I_{sd} recovers for FET-1 but not for FET-2. Indeed, P3HT of FET-2 is so seriously damaged that the current can never be fully recovered by doping. After thermal de-doping in Procedure 2–13, the I_{sd}, on/off-current ratio, and mobilities all go back to the values before the photo-induced O_2 doping in Procedure 2–10. This illustrates that although P3HT are damaged, the O_2 doping process is still totally reversible under normal photon energy, intensity, O_2 pressure, and temperature ranges. The mobility and on/off-current ratio results are plotted in Fig. 2(d) via different procedures and are summarized in Table III.

C. Doping and light wavelength

Except for the 405 nm laser, so far the light employed for photo-induced O_2 doping is derived from a lamp with broad emission spectrum. It is important to know the range of the wavelength that causes the majority of the doping since they should be avoided in the sample fabrication in order to reduce the undesired off-current. Red light in the 600–700 nm range has been shown to enhance the oxygen doping, but the study is not extended into the shorter wavelength spectral region that overlaps with the absorption spectrum of P3HT. Below we study the wavelength dependence of the efficiency of the doping for the wide range of wavelengths covering the near infrared and the whole visible range. Such doping spectrum is also crucial to understanding the mechanism of the photo-induced doping which renders the high sensitivity of P3HT to the ambient light during sample fabrication where t is time and np is the relative photon flux from the lamp for a given wavelength.

The doping efficiency is defined as the I_{sd} increment per unit time and per unit photon flux $\Delta I_d/(\Delta t n_p)$. In Fig. 3 $\Delta I_d/(\Delta t n_p)$ is plotted against the wavelength selected by a monochromator under 47 torr O_2 atmosphere. Positive $\Delta I_d/\Delta t n_p$ means the light-induced O_2 doping rate is larger than the O_2 desorption rate. From Fig. 3, cases of incident light with wavelength larger than 680 nm all have small and negative $\Delta I_d/\Delta t n_p$ values. When the wavelength is below 680 nm $\Delta I_d/\Delta t n_p$ becomes positive and has a peak at 610 nm. The 500–600 nm photons within the absorption range dose enhance the O_2 doping process. The doping spectrum is, however, very different from the absorption spectrum, which is shown for comparison. To confirm the I_{sd} increase is not the photocurrent from the interband absorption and the reversibility of photo-induced oxygen doping process, two two-terminal devices (SD-3 and SD-4) on the same substrate are compared, as shown in the inset of Fig. 3. SD-3 is di-

TABLE III. Time-correlated on/off ratio and mobility of FET devices at different experimental conditions.

Procedure	Time interval (min)	Light	Temperature (K)	O_2	FET-1 Initial on/off ratio	FET-1 Final on/off ratio	FET-1 Mobility (10^{-4} cm^2/Vs)	FET-2 Initial on/off ratio	FET-2 Final on/off ratio	FET-2 Mobility (10^{-4} cm^2/Vs)
1(start)	0	Dark	300	Vacuum	23	—	18.2	22	—	22.3
2	0–146	Dark	370 for 2 h	Vacuum	23	114.6	11.5	22	105	9.5
3	146–197	Dark	300	650 torr	114.6	103.7	9.74	105	100	8.6
4	197–230	Dark	300	Vacuum	—	—	—	—	—	—
5	230–240	Light	300	125 torr	—	8.5	12.6	—	6.8	9.9
6	240–259	Dark	300	Vacuum	8.5	19	8.5	6.8	17	8.7
7	259–400	Dark	370 for 2 h	Vacuum	19	93.6	12.4	17	70.8	7.9
8	400–476	Laser on FET-2	300	136 torr	93.6	4.3	15.4	70.8	1.14	5.8
9	476–1200	Dark	300	Vacuum	4.3	22	13	1.14	1.75	2.4
10	1200–1404	Dark	370 for 2 h	Vacuum	22	66	7.56	2.68	1.75	0.38
11	1404–1421	Light	300	130 torr	66	8	9.31	1.75	1.7	0.61
12	1421–1432	Dark	300	130 torr	—	—	—	—	—	—
13	1432–1650	Dark	370 for 2 h	130 torr	8	62	8.42	1.7	2.78	0.34

rectly illuminated by a focused monochromatic light, and SD-4 is only affected by weak scattered light from SD-3. I_{sd} of SD-3 under the direct 500 nm light illumination in 47 torr O_2 atmosphere increases with time, while I_{sd} of SD-4 remain constant. After I_{sd} of SD-3 is increased by 15%, the incident light is stopped and the sample is returned to the dark with the same O_2 pressure. The increased I_{ds} of SD-3 does not disappear rapidly but is gradually reduced with time and back to the initial current levels after tens of minutes. The slow recovery suggests desorption of O_2 molecules from P3HT so the increased I_{sd} is not due to the photocurrent from P3HT band-gap absorption, which would disappear immediately after light is turned off. This photo-induced O_2 doping effect is reversible for the 500 nm wavelength. The major difference between the doping and absorption spectra is that the doping spectrum is more pronounced in the long wavelength region and decreases rapidly for wavelength below 610 nm where the absorption increases. The spectral difference together with the long transient time indicates that the excitation is not the simple interband transition but a new excited state that does not exist in pure P3HT. In other words, the electronic structure of P3HT is modified by the adsorption of the molecular oxygen despite that no irreversible chemical reaction takes place. It has been shown by *ab initio* calculation that adsorption of oxygen on a carbon nanotube changes the electronic structure from a semiconductor to a metal through the hybridization of oxygen and carbon wave functions.[23] A nearly half-filled oxygen band forms by the hybridization with Fermi level pinned within. Even in the ground state there is a net electron transfer from the polymer to the oxygen band to cause a *p*-doping. Recently it was shown theoretically that similar semiconductor-metal transition happens for conjugated polymers with oxygen adsorption as well.[18] The doping peak at 610 nm in Fig. 3 is presumably due to the transition from the filled and flat sulfur-dominated band to the nearly half-filled flat oxygen band. The net result is an electron transfer from P3HT to O_2 to form a complex. Under the applied electric field the hole in P3HT is driven away from the oxygen and a carrier is created. The existence of free holes may also enhance the adsorption of oxygens by acting as an oxygen trap to form a meta-stable complex. Note that there are two ways to create hole carriers by oxygen. One is the dark doping through the wave function hybridization, the other is the photo-doping through the creation of the complex. From the dynamics the efficiency of the photo-doping is much higher than the dark doping, but both of them are reversible under thermal annealing.

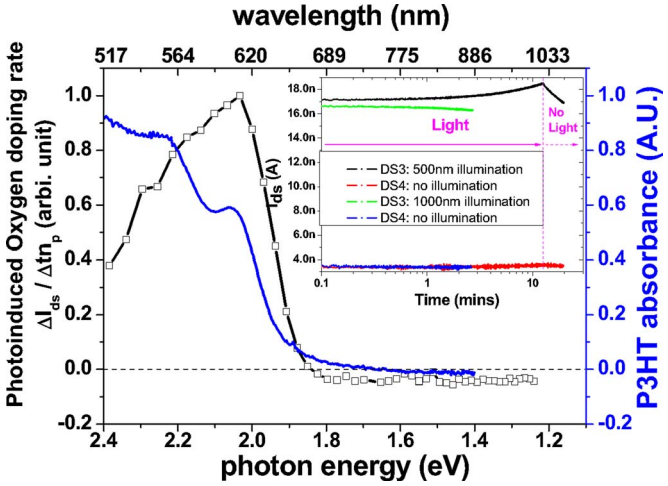

FIG. 3. (Color online) The photo-induced oxygen doping rate spectroscopy. ΔI_{ds} is the dark current I_{ds} increment per unit time Δt divided by total incident photon numbers n_p in arbitrary units. The sample is a DS two-terminal device. The inset is the time evolution of the I_{ds} of two source-drain devices DS3 and DS4. DS3 is directly illuminated by the monochromatic light beam, DS4 is not.

D. Dynamic picture of doping and de-doping

From the doping/de-doping dynamics and reversibility above a picture of the interaction between oxygen molecules and P3HT is established. The state of the polymer is controlled by the dynamics of the oxygen adsorption and desorption processes (Fig. 4). For adsorption the oxygen molecules

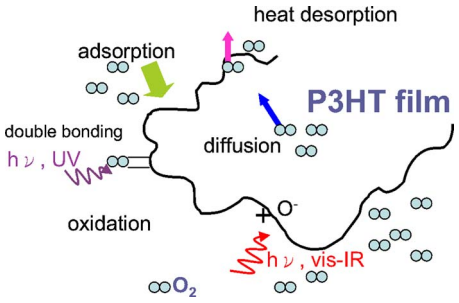

FIG. 4. (Color online) The physical picture of the oxygen adsorption doping process. The physical state of the P3HT is determined by the continuous oxygen adsorption and desorption whose rates are controlled by factors including oxygen pressure, temperature, and light. Adsorption occurs either slowly through diffusion in the dark or accelerated by the vis-IR light, which creates a polymer-oxygen complex. Deep blue and UV light will cause photo-oxidation and irreversible degradation of the polymer carrier mobility. Oxygen desorption occurs slowly at room temperature by diffusion out of the polymer matrix. Once the polymer is heated above the glass temperature, the desorption rate is significantly accelerated due to chain motions.

need to diffuse through the polymer matrix followed by the capture upon the polymer chains, which is significantly enhanced by the creation of polymer-oxygen complex by light around 610 nm. For UV light in addition to adsorption enhancement the chemical structure of the polymer is damaged by the illumination, resulting in mobility degradation and current irreversibility. Diffusion also causes desorption from the polymer, with rate depending significantly on temperature. In general it is quite difficult for the adsorption and desorption processes to reach an equilibrium since both of them are slow processes, especially without light. At room temperature without light, as a previously doped sample is placed in a vacuum with the oxygen pressure lower than 10^{-4} torr, the desorption continues for over 24 h. On the other hand, as the fully de-doped sample is placed in a 650 torr oxygen environment, the adsorption continues for several days before it reaches the heavy doping level. Only with light the adsorption is dramatically shortened to within a few minutes. This indicates that in order to avoid doping during sample fabrication, light in the visible and near infrared range must be under strict control. The desorption process is accelerated from several days to a few hours as the temperature is raised from room temperature to 370 K. Since the kinetic energy of the oxygen molecules does not change too much in this temperature range, the acceleration of desorption is attributed to the chain motion of the polymers. Indeed, 370 K is close to the glass temperature of P3HT where the chains are allowed to move so the trapped oxygen can be released if the pressure outside the matrix is low. As stressed above, no matter if the doping takes place in the dark slowly or with light rapidly, the doping can always be removed by the thermal annealing process with mobility largely unaffected unless the light is from a UV laser. This remarkably robust reversibility is helpful for the fabrication of polymer electronics because the doping caused by exposure to air and ambient light can be eventually removed before encapsulation.

IV. CONCLUSION

In conclusion, through real-time monitoring of the electrical characteristics under changing external conditions, the *p*-doping of high carrier mobility polymer poly(3-hexyl thiophene) is shown to be controlled by the complex adsorption and desorption processes with time scales ranging from minutes to as long as a week. The doping by oxygen adsorption is limited by the slow diffusion through the polymer matrix in the dark and takes several days to reach the heavy doping level. As light in the 500 to 700 nm range is introduced to the polymer the doping process is dramatically accelerated from days to minutes, even at very low oxygen pressure. Creation of polymer-oxygen complex by the optical transition from sulfur band to oxygen band in the hybridized system is believed to be the microscopic mechanism. On the other hand, the de-doping by oxygen desorption is also very slow at room temperature and takes a few days to reach a nearly intrinsic doping level, apparently also limited by the slow diffusion out of the polymer matrix. As the temperature is raised to near the polymer glass temperature, the de-doping is accelerated to several hours due to the enhanced chain motion, which releases the trapped oxygen. The whole doping and de-doping procedures can be repeated indefinitely and are fully reversible. Only the carrier density is changed while the mobility remains roughly a constant. In order to create irreversible damage to the polymer a UV laser has to be focused on the polymer in the presence of oxygen. Mobility is then degraded by the photo-oxidation and the current can no longer be recovered in subsequent process. These results indicate ultraviolet light must be avoided during the fabrication of polymer electronic devices. Visible and near infrared light do cause very efficient doping within a minute during fabrication, even at a medium vacuum level. But such doping is fully reversible by thermal annealing at the end without sacrificing the mobility. Despite the high oxygen and light sensitivity, the manufacturing process does not need to be strictly controlled since they do not inflict irreversible damage.

ACKNOWLEDGMENTS

This work was supported by the National Science Council of Taiwan, the Republic of China. (Grant No. NSC96-2112-M-009-036).

[1]H. F. Meng, C. C. Liu, C. J. Jiang, Y. L. Yeh, S. F. Horng, and C. S. Hsu, Appl. Phys. Lett. **89**, 243503 (2006).
[2]G. Li, V. Shrotriya, J. Huang, Y. Yao, T. Moriarty, K. Emery, and Y. Yang, Nat. Mater. **4**, 864 (2005).
[3]Y. Kim, S. Cook, S. M. Tuladhar, S. A. Choulis, J. Nelson, J. R. Durrant, D. D. C. Bradley, M. Giles, I. McCulloch, C. S. Ha, and M. Ree, Nat. Mater. **5**, 197 (2006).
[4]B. A. Mattis, P. C. Chang, and V. Subramanian, Synth. Met. **156**, 1241 (2006).
[5]S. M. Sze, *Physics of Semiconductor Devices*, 2nd ed. (Central Book, Taiwan, 1983), Chap. 14, p. 794.
[6]T. D. Anthopoulos and T. S. Shafai, Thin Solid Films **441**, 207 (2003).
[7]M. S. A. Abdou, F. P. Orfino, Y. Son, and S. Holdcroft, J. Am. Chem. Soc. **119**, 4518 (1997).
[8]M. S. A. Abdou, F. P. Orfino, Z. W. Xie, M. J. Deen, and S. Holdcroft, Adv. Mater. **6**, 838 (1994).
[9]S. Hoshino, M. Yoshida, S. Uemura, T. Kodzasa, N. Takada, T. Kamata, and K. Yase, J. Appl. Phys. **95**, 5088 (2004).
[10]G. Horowitz, X. Peng, D. Fichou, and F. Garnier, J. Appl. Phys. **67**, 528 (1990).
[11]E. J. Meijer, C. Detcheverry, P. J. Baesjou, E. van Veenendaal, D. M. de Leeuw, and T. M. Klapwijk, J. Appl. Phys. **93**, 4831 (2003).

[12]S. Ogawa, T. Naijo, Y. Kimura, H. Ishii, and M. Niwano, Jpn. J. Appl. Phys., Part 1 **45**, 530 (2006).
[13]E. J. Meijer, A. V. G. Mangnus, B. H. Huisman, G. W. t Hooft, D. M. de Leeuw, and T. M. Klapwijk, Synth. Met. **142**, 53 (2004).
[14]T. D. Anthopoulos and T. S. Shafai, Appl. Phys. Lett. **82**, 1628 (2003).
[15]B. van der Zanden and A. Goossens, J. Appl. Phys. **94**, 6959 (2003).
[16]Y. Y. Noh, D. Y. Kim, and K. Yase, J. Appl. Phys. **98**, 074505 (2005).
[17]Y. Y. Noh, J. Ghim, S. J. Kang, K. J. Baeg, D. Y. Kim, and K. Yase, J. Appl. Phys. **100**, 094501 (2006).
[18]C. K. Lu and H. F. Meng, Phys. Rev. B **75**, 235206 (2007).
[19]T. Nishi, K. Kanai, Y. Ouchi, M. R. Willis, and K. Seki, Chem. Phys. **325**, 121 (2006).
[20]V. Derycke, R. Martel, J. Appenzeller, and Ph. Avouris, Appl. Phys. Lett. **80**, 2773 (2002).
[21]D. B. A. Rep, A. F. Morpurgo, W. G. Sloof, and T. M. Klapwijk, J. Appl. Phys. **93**, 2082 (2003).
[22]R. Payerne, M. Brunb, P. Rannoua, R. Baptistb, and B. Grevina, Synth. Met. **146**, 311 (2004).
[23]S. H. Jhi, S. G. Louie, and M. L. Cohen, Phys. Rev. Lett. **85**, 1710 (2000).